JOURNAL OF SOLID STATE CHEMISTRY **125,** 165–170 (1996)
ARTICLE NO. 0280

Mo_2 Dimers in $[Mo(Te_2)_2]$ Chains in $MoTe_4Br$ and in their Cationic Fragments $[Mo_2(Te_2)_2(Te_4)_2]^{6+}$ in $MoTe_6Br_3$: Two Molybdenum Telluride Bromides with a Close Structural Relationship

Johannes Beck[1]

Institut für Anorganische und Analytische Chemie, Justus-Liebig-Universität, Heinrich-Buff-Ring 58, D-35392 Gießen, Germany

Received February 21, 1996; in revised form May 14, 1996; accepted May 16, 1996

$MoTe_4Br$ is obtained from Te_2Br and $MoTe_2$ in a sealed evacuated silica ampoule at 440°C in the form of platelike crystals with a silver luster. It crystallizes in the triclinic space group $P\bar{1}$ with $a = 682.1(3)$ pm, $b = 783.6(3)$ pm, $c = 793.1(3)$ pm, $\alpha = 113.25(2)°$, $\beta = 102.97(1)°$, $\gamma = 101.37(2)°$. The structure is built of infinite one-dimensional $Mo(Te_2)_2$ chains with intercalated bromide ions and Mo_2 pair formation along the chain. $MoTe_6Br_3$ is formed from $MoBr_3$, Te_2Br, and Te in 1 : 2 : 2 molar ratio in a sealed evacuated glass ampoule at 300°C. The silvery crystals belong to the triclinic crystal system, space group $P\bar{1}$, $a = 837.2(1)$ pm, $b = 1141.4(2)$ pm, $c = 1442.0(2)$ pm, $\alpha = 81.70(1)°$, $\beta = 83.07(1)°$, $\gamma = 74.34(1)°$. The structure consists of dimeric cationic complexes $[Mo_2(Te_2)_2(Te_4)_2]^{6+}$ which are connected by bromide ions to layers. In the complexes Mo_2 pairs are bridged by two Te_2^{2-} groups and are additionally bound in a η^4–π fashion to two almost planar Te_4 rings that can be considered to be Te_4^{2+} polycations. The complexes in the structure of $MoTe_6Br_3$ can formally be derived as fragments from the chains of $MoTe_4Br$.

INTRODUCTION

The elements of group 6, chromium, molybdenum, and tungsten, form a well-characterized series of chalcogenide halides with oxygen, sulfur, and selenium (1). Many of these ternary compounds contain terminal $M = E$ groups (M = Mo, W; E = O, S, Se) with a formal metal–chalcogen double bond. Often isotypic series exist, in which the different chalcogens or halogens can replace each other without changing the structure type. These series always cease with the selenide halides. Telluride halides of chromium are unknown and for molybdenum the only known telluride halides derive from the cluster compounds of Mo(II) (2, 3). The same holds for tungsten. With the exception of the one-dimensional chain compound $W_2O_2Te_4Br_5$ tungsten telluride halides are unknown (4). This subject has recently been reviewed (4). In this article the syntheses and crystal structures of the molybdenum telluride bromides $MoTe_4Br$ and $MoTe_6Br_3$, containing a very uncommon Te_4^{2+} ligand attached to the metal in a η^4–π fashion, are described. The structural relation between the two compounds is discussed.

EXPERIMENTAL

Synthesis of $MoTe_4Br$. A silica ampoule of 15 cm length and 1.5 cm diameter is filled with 1.5 g (4.3 mmol) $MoTe_2$ (5) and 1.43 g (4.3 mmol) Te_2Br (6). The ampoule is evacuated and sealed, and placed in a horizontal tube furnace with a temperature gradient 500 → 400°C. In the 440°C zone silvery platelike crystals of $MoTe_4Br$ are deposited within 3 weeks.

Synthesis of $MoTe_6Br_3$. A silica ampoule of identical dimensions is charged with 0.5 g (1.5 mmol) $MoBr_3$, 1 g (3 mmol) Te_2Br, and 0.38 g (3 mmol) Te. The ampoule is evacuated and sealed, and placed in a horizontal tube furnace with a temperature gradient 340 → 270°C. In the hot part of the ampoule $MoTe_6Br_3$ is formed within 4 weeks in the form of silvery crystals that occur mainly as spherical agglomerates.

Structure determinations. Crystals of $MoTe_4Br$ are very easily cleaved into fibers and much care had to be taken to separate an undistorted crystal from the reaction ampoule. All examined crystals show broad, curved reflections on X-ray photographs. No symmetry higher than $\bar{1}$ was detected; the triclinic space group $P\bar{1}$ was confirmed through the structure analysis. A crystal in the form of a thin plate with the dimensions $0.27 \times 0.16 \times 0.02$ mm was selected for data collection. Due to the broad reflections a scanwidth of $\Delta\omega = 3°$ was necessary.

The selected crystal of $MoTe_6Br_3$ with the dimensions $0.23 \times 0.20 \times 0.09$ mm showed no symmetry higher than $\bar{1}$ on preliminary photographs; the space group $P\bar{1}$ was confirmed through the structure analysis.

[1] To whom correspondence should be addressed.

0022-4596/96 $18.00

TABLE 1
Crystallographic Data, Data Collection, and Structure Refinement for $MoTe_4Br$ and $MoTe_6Br_3$

	$MoTe_4Br$	$MoTe_6Br_3$
Crystal system	triclinic	triclinic
Space group	$P\bar{1}$	$P\bar{1}$
Unit cell dimensions	a = 682.1(3) pm	a = 837.2(1) pm
	b = 783.6(3) pm	b = 1141.4(2) pm
	c = 793.1(3) pm	c = 1442.0(2) pm
	α = 113.25(2)°	α = 81.70(1)°
	β = 102.97(1)°	β = 83.07(1)°
	γ = 101.37(2)°	γ = 74.34(1)°
Volume	359.8 × 10^6pm^3	1308.1 × 10^6pm^3
Z	2	4
Density (calc.)	6.33 Mg/m^3	5.59 Mg/m^3
Absorption coefficient	21.9 mm^{-1}	22.1 mm^{-1}
F(000)	570	1836
Diffractometer	STOE AED 2	STOE AED 2
Radiation	MoK_α(λ = 71.073 pm)	MoK_α(λ = 71.073 pm)
Temperature	294(K)	294(K)
Monochromator	graphite crystal	graphite crystal
2 θ range	5.0 to 60.0°	2.0 to 50.0°
Scan type	ω-scan	ω/θ-scan
Reflections collected	4196	9121
Independent reflections	2098 (R_{int} = 0.030)	4591 (R_{int} = 0.022)
Observed reflections	1807 [$F > 2\sigma(F)$]	4345 [$F > 2\sigma(F)$]
Absorption correction	numerical, description of the crystal shape by 6 faces	numerical, description of the crystal shape by 14 faces
Transmission factors	0.668 to 0.078	0.240 to 0.044
Refined parameters	56	181
Data to parameter ratio	32:1	25:1
R indices	$R(R_w)$ = 0.047(0.044)	$R(R_w)$ = 0.022(0.021)
Weighting scheme	$w = [\sigma^2(F)]^{-1}$	$w = [\sigma^2(F)]^{-1}$
Largest peak	2.72 e/10^6pm^3	1.49 e/10^6pm^3
Largest hole	−3.88 e/10^6pm^3	−1.67 e/10^6pm^3

Both structures were solved by direct methods (7) and refined with the aid of full matrix least squares techniques (8). Crystallographic data and details of data collection and refinement are given in Table 1. Atomic positional parameters are presented in Tables 2 and 3 and selected bond lengths are found in Tables 4 and 5.

Magnetism of $MoTe_4Br$. The magnetic susceptibility of $MoTe_4Br$ was determined on a 363.2 mg sample over the temperature range 5–310 K using a Quantum Design SQUID susceptometer.

TABLE 2
Atomic Coordinates and Equivalent Isotropic Displacements Coefficients (10^4pm^2) for $MoTe_4Br$.

	x	y	z	$B_{(eq)}$
Mo	0.2199(2)	0.0004(2)	−0.0017(2)	0.91(8)
Te(1)	0.1215(1)	0.3339(1)	0.1744(2)	1.35(6)
Te(2)	−0.0374(1)	0.1130(2)	−0.2295(1)	1.41(7)
Te(3)	0.4605(1)	−0.2396(1)	0.0637(2)	1.34(7)
Te(4)	0.6118(1)	0.1438(1)	0.3131(1)	1.38(6)
Br	0.2582(1)	0.3948(3)	0.5901(3)	2.3(1)

TABLE 3
Atomic Coordinates and Equivalent Isotropic Displacement Coefficients (10^4pm^2) for $MoTe_6Br_3$

	x	y	z	$B_{(eq)}$
Mo(1)	0.46954(7)	0.12124(6)	0.53380(3)	1.03(3)
Mo(2)	−0.02753(7)	0.37846(6)	0.03583(3)	1.05(3)
Te(1)	0.64839(6)	0.06483(5)	0.36707(3)	1.57(3)
Te(2)	0.77339(6)	−0.04639(5)	0.53428(3)	1.65(3)
Te(3)	0.53256(6)	0.19527(5)	0.69939(3)	1.95(3)
Te(4)	0.64883(6)	0.30260(5)	0.53054(3)	1.95(3)
Te(5)	0.33025(6)	0.36161(5)	0.45677(3)	1.83(3)
Te(6)	0.20721(6)	0.28223(5)	0.63353(3)	1.92(3)
Te(7)	−0.13633(7)	0.57428(5)	0.13537(3)	2.13(3)
Te(8)	0.19987(6)	0.46959(5)	0.10390(3)	2.23(3)
Te(9)	0.17736(7)	0.14106(5)	0.05806(4)	2.53(3)
Te(10)	−0.03158(7)	0.22862(5)	0.21082(3)	2.25(3)
Te(11)	−0.30624(6)	0.29302(5)	0.10670(4)	2.55(3)
Te(12)	−0.10196(8)	0.18519(5)	−0.04105(3)	2.62(3)
Br(1)	0.8788(1)	0.1115(1)	0.71764(6)	3.34(6)
Br(2)	0.0154(1)	0.37826(9)	0.40171(6)	3.31(6)
Br(3)	0.6131(1)	0.41246(9)	0.29953(5)	3.12(6)
Br(4)	0.2608(1)	0.08543(9)	−0.15306(5)	3.12(6)
Br(5)	0.6415(1)	−0.17003(9)	0.76545(5)	2.76(5)
Br(6)	0.5042(1)	0.3290(1)	−0.07818(6)	3.47(6)

RESULTS AND DISCUSSION

$MoTe_4Br$ is obtained from the reaction of $MoTe_2$ and Te_2Br in equimolar ratio in a chemical transport reaction. The use of air stable $MoTe_2$ (5) and Te_2Br (6) is convenient but the synthesis also succeeds from a mixture of the elements (9) or from Mo, Te, and $TeBr_4$. $MoTe_4Br$ is deposited from the vapor phase as air stable, plate and needle shaped crystals with a bright silver luster. The crystals are very easily bent and cleaved into fibers. These mechanical properties already hint at the one-dimensional structure. The crystals loose their silver luster on mechanical treatment and leave a black fibrous powder.

The structure of $MoTe_4Br$ consists of infinite one-dimensional $Mo(Te_2)_2$ chains with intercalated bromide ions. Fig-

TABLE 4
Selected Bond Lengths (pm) in $MoTe_4Br$

Mo–Mo^{I}	300.5(2)	Te(3)–Te(4)	267.8(1)
Mo–Mo^{II}	381.6(2)	Te(1^{I})–Te(2)	364.8(1)
Mo–Te(1)	273.2(1)	Te(3)–Te(4^{I})	331.6(1)
Mo–Te(2)	275.1(2)	Te(1)–Br	302.8(2)
Mo–Te(3)	284.7(1)	Te(4^{III})–Br	327.0(2)
Mo–Te(4)	287.2(1)	Te(3^{IV})–Br	344.1(2)
Te(1)–Te(2)	278.5(1)	Te(2^{I})–Br	360.5(2)
		Te(2^{V})–Br	360.9(2)

Note. Symmetry operations: I, $-x$, $-y$, $-z$; II, $-x+1$, $-y$, $-z$; III, $-x+1$, $-y+1$, $-z+1$; IV, x, $y+1$, $z+1$.

TABLE 5
Selected Bond Lengths (pm) in $MoTe_6Br_3$

Mo(1)–Mo(1^{I})	296.1(1)	Mo(2)–Mo(2^{II})	295.4(1)
Mo(1)–Te(1)	273.8(1)	Mo(2)–Te(7)	272.0(1)
Mo(1)–Te(2)	273.9(1)	Mo(2)–Te(8)	273.6(1)
Mo(1)–Te(1^{I})	272.8(1)	Mo(2)–Te(7^{II})	273.2(1)
Mo(1)–Te(2^{I})	273.7(1)	Mo(2)–Te(8^{II})	273.7(1)
Mo(1)–Te(3)	279.7(1)	Mo(2)–Te(9)	278.6(1)
Mo(1)–Te(4)	285.9(1)	Mo(2)–Te(10)	283.9(1)
Mo(1)–Te(5)	279.7(1)	Mo(2)–Te(11)	279.4(1)
Mo(1)–Te(6)	284.4(1)	Mo(2)–Te(12)	284.6(1)
Te(1)–Te(2)	274.4(1)	Te(7)–Te(8)	275.5(1)
Te(3)–Te(4)	275.4(1)	Te(9)–Te(10)	277.0(1)
Te(4)–Te(5)	286.5(1)	Te(10)–Te(11)	277.2(1)
Te(5)–Te(6)	275.4(1)	Te(11)–Te(12)	277.8(1)
Te(6)–Te(3)	286.3(1)	Te(12)–Te(9)	278.0(1)
Te(3)–Br(1)	282.8(1)	Te(9)–Br(4)	315.7(1)
Te(3)–Br(4^{IV})	329.8(1)	Te(9)–Br(5^{II})	321.4(1)
Te(4)–Br(1)	361.0(1)	Te(10)–Br(3)	337.3(1)
Te(4)–Br(3)	340.4(1)	Te(10)–Br(5^{II})	320.2(1)
Te(5)–Br(2)	279.4(1)	Te(11)–Br(3)	319.2(1)
Te(5)–Br(3)	318.6(1)	Te(11)–Br(6^{III})	318.5(1)
Te(6)–Br(2)	377.4(1)	Te(12)–Br(4)	325.7(1)
Te(6)–Br(4^{IV})	353.7(1)	Te(12)–Br(6^{III})	333.2(1)

Note. Symmetry operations: I, $-x + 1, -y, -z + 1$; II, $-x, -y + 1, -z$; III, $x - 1, y, z$; IV, $x, y, z + 1$.

ure 1 shows the unit cell in a perspective view along the chains and Fig. 2 a section of one of the chains. $MoTe_4Br$ is isotypic with $TaTe_4I$, which is closely related to $NbTe_4I$ (10). Each Mo atom is coordinated by eight Te atoms in the form of a nearly regular square antiprism. The antiprism is built of four Te_2^{2-} groups with markedly different Te–Te

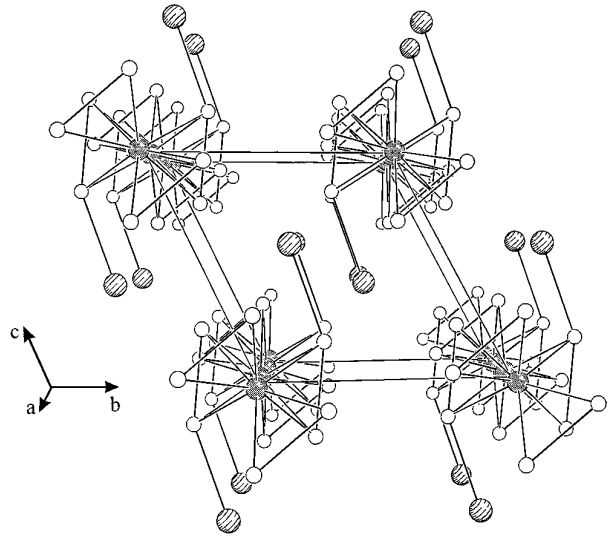

FIG. 1. View of the structure of $MoTe_4Br$ down *a*, showing the packing of the chains. Dotted circles, Mo; striped circles, Br; open circles, Te.

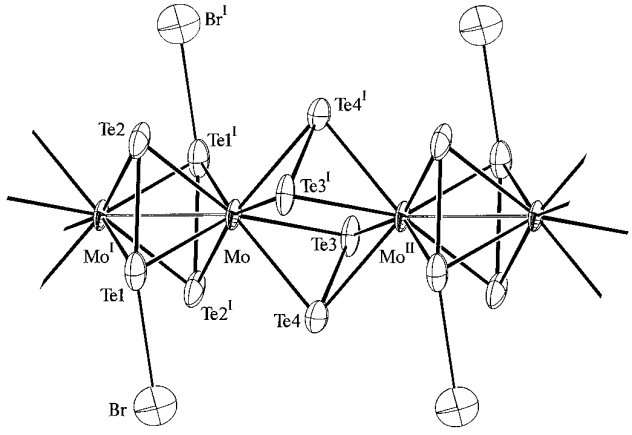

FIG. 2. Section of a $(MoTe_4Br)_n$ chain. The thermal ellipsoids are scaled to enclose a 90% probability density.

distances of Te(1)–Te(2) 278.5(1) pm and Te(3)–Te(4) 267.8(1) pm. Along the other prism edges Te–Te distances in the nonbonding range (Te(1^{I})–Te(2) 364.8(1) pm) or only weakly bonding range (Te(3)–Te(4^{I}) 331.6(1) pm) are found. The Mo–Te bonds also differ considerably. The Te(1)–Te(2) group with the longer Te–Te distance forms short Mo–Te bonds of 273.2(1) and 275.1(2) pm, while the Te(3)–Te(4) dumb-bell forms longer Mo–Te bonds of 284.7(1) and 287.2(1) pm. Along the chain Mo_2 pair formation occurs. The short Mo–Mo^{I} contact of 300.5(2) pm is still within the range of metal–metal bonding; the long distance between Mo and Mo^{II} of 381.6(2) pm cannot be considered as a metal–metal interaction. The Mo_2 pair formation shows that the Mo atoms still possess *d* electrons. The bromide ions in the structure of $MoTe_4Br$ form close contacts to several Te atoms, of which the Te(1)–Br distance of 302.8(2) pm is shortest. For a covalent Te–Br bond a length of about 250 pm is expected, so a bond of 303 pm is very weak but still partially covalent (11). The Te–Br distances in the tellurium subhalide Te_2Br of 290 and 302 pm are in the same range (6). Extended Hückel band structure calculations (13) show for $MoTe_4Br$ small (max. 0.07) but significant positive Te(1)–Br overlap populations. Whether the distance between Te(1) and Br is regarded as a covalent Te–Br bond, or as a close contact of a Br^- ion with a positively charged $Mo(Te_2)_2$ chain, results in two different ionic formulas for $MoTe_4Br$.

Assuming an isolated Br^- ion, Mo is coordinated by two Te_2^{2-} groups and carries the formal charge +5 : $[(Mo^{5+})(Te_2^{2-})_2)]^+Br^-$. Assuming a covalent Te–Br bond, $MoTe_4Br$ contains an anionic Te_2Br^- group and Mo carries the formal charge +3: $(Mo^{3+})(Te_2^{2-})(Te_2Br^-)$. A determination of the magnetic properties could not help to reach a decision for one of the two possibilities. $MoTe_4Br$ shows only a weak, nearly temperature-independent paramagnetism with a magnetic moment of 0.1 μ_B at 15 K which slowly

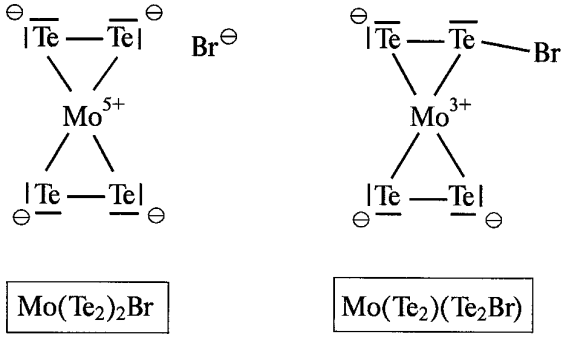

FORMULA 1

increases to 0.4 μ_B at 310 K. This indicates a very strong coupling of the unpaired electrons. The comparison with the structurally closely related $TaTe_4I$ favors the existence of Mo^{5+}ions with a d^1 configuration. In $TaTe_4I$ the oxidation state of Ta certainly is +5, because no Ta–Ta pairs are present; instead a nearly equidistant chain of Ta atoms is formed. On the other hand significant Te–Te bond lengthening of those Te_2 groups taking part in the short Te–halogen contacts is observed in both structures. In $TaTe_4I$ this difference between the two sorts of Te_2 groups is 4 pm, while in $MoTe_4Br$ the bond length increase is 11 pm. This shows that the Te–Br interaction in $MoTe_4Br$ is slightly bonding and lends weight to the interpretation of a Te_2Br^- group. The Te_2Br fragment has already been found in $[(C_5H_5)(CO)_2MoFe(CO)_3(Te_2Br)]$ (14). Here the Te–Te and the Te–Br distances are both 281 pm. This complex is only weakly dissociated in solution, which indicates the strength of the relatively short Te–Br bond. With $AgSbF_6$, however, this complex reacts to give the 1 : 1 electrolyte $[(C_5H_5)(CO)_2MoFe(CO)_3(Te_2)]^+$ SbF_6^- under cleavage of the Te–Br bond.

$MoTe_6Br_3$ is obtained only in the presence of an excess of bromine. $MoBr_3$, Te_2Br, and Te in a 1 : 2 : 2 ratio, corresponding to a composition Mo/6Te/5Br, react in a temperature gradient 340 → 270°C to silvery, air stable crystals in the hot zone of the ampoule. A black melt of mainly Te and $TeBr_4$ is always present in the cold end of the ampoule. After 4 weeks the material in the hot end is transformed quantitatively to $MoTe_6Br_3$. With a lower excess of bromine the formation of $MoTe_4Br$ is favored and temperatures higher than 350°C cause the decomposition into $MoTe_4Br$. No conditions for a long range vapor transport could be found so far for $MoTe_6Br_3$.

The unit cell of $MoTe_6Br_3$ contains 12 bromide ions and two crystallographically independent but nearly isostructural dinuclear cationic complexes (Fig. 3). Each complex contains Mo_2 pairs with Mo–Mo distances of 296.1(1) and 295.4(1) pm, slightly less than in $MoTe_4Br$ and within the range of metal–metal bonding. The Mo_2 pairs in each complex are bridged by two Te_2 groups with Te–Te bonds of 274.4(1) and 275.5(1) pm as expected for Te–Te single bonds. Two almost planar Te_4 rings, bound in an η^4–π fashion, complete the coordination of each Mo atom to a square antiprismatic environment. The bonds between Mo atoms and the Te_2 dumb-bells are in a narrow range between 272.0(1) and 273.7(1) pm; those between Mo and Te atoms of the Te_4 rings are in a broader range between 278.6(1) and 285.9(1) pm. The Te_4 rings of complex I are distorted to rectangles. The Te–Te bonds between Te(3)–Te(4) and Te(5)–Te(6) of each 275.4(1) pm are shorter than Te(4)–Te(5) 286.5(1) pm and Te(3)–Te(6) 286.3(1) pm. The Te_4 rings of complex II are more regular with Te–Te bond lengths in the range of single bonds between 277.0(1) and 278.0(1) pm. If the Te_4 rings are assumed to be complexing Te_4^{2+} polycations the ionic formulation for $MoTe_6Br_3$ would be $[(Mo^{3+})_2(Te_2^{2-})_2(Te_4^{2+})_2]^{6+}(Br^-)_6$. Only a few examples for chalcogen-polycations acting as complex ligands are known. $Mo(CO)_6$ or $W(CO)_6$ react with

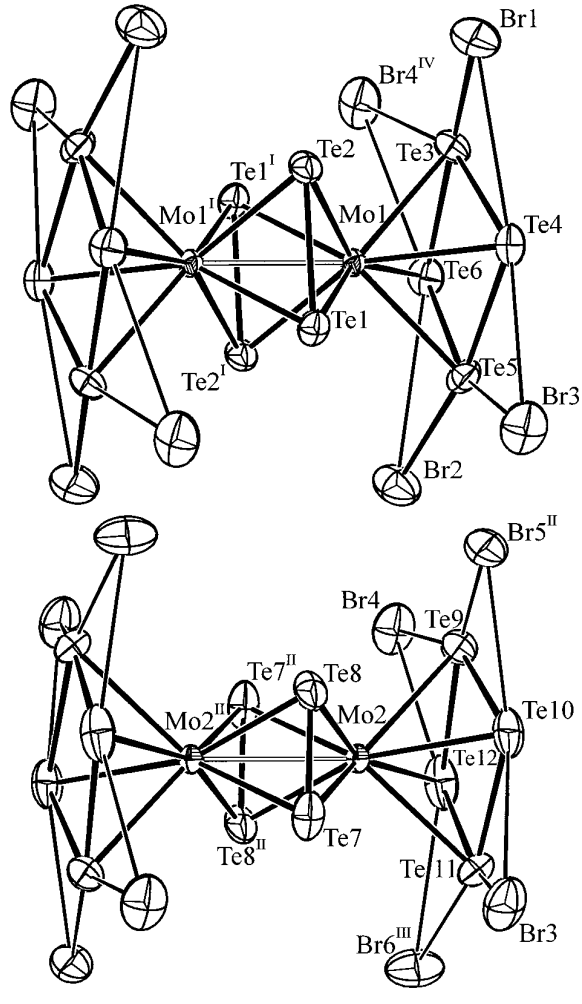

FIG. 3. The two symmetrically independent centrosymmetric complexes in the structure of $MoTe_6Br_3$ (on top complex I, on bottom complex II). All Br atoms with Te–Br distances up to 360 pm are included. The thermal ellipsoids are scaled to enclose a 70% probability density.

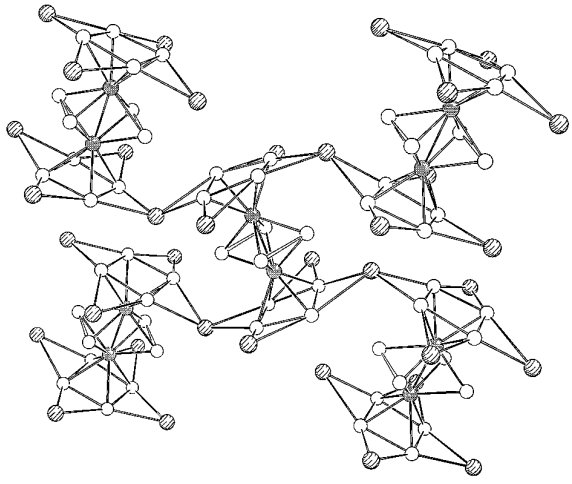

FIG. 4. The connection of $[Mo_2(Te_2)_2(Te_4)_2]^{6+}$ complexes to layers by joint Br^- ions in the structure of $MoTe_3Br_6$.

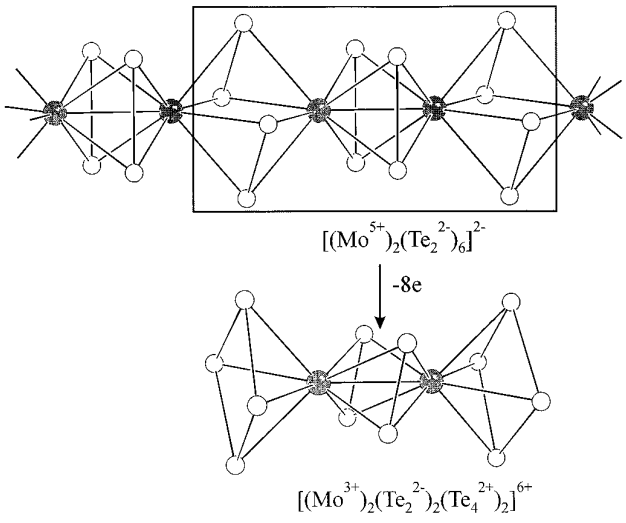

FIG. 5. A section of a chain in the structure of $MoTe_4Br$. Bromide ions are omitted. The fragment in the frame corresponds to the formula $[Mo_2(Te_2)_6]^{2-}$. The formal oxidation leads to the cationic complex $[Mo_2(Te_2)_2(Te_4)_2]^{6+}$ in the structure of $MoTe_6Br_3$.

Se_4^{2+} in liquid SO_2 to the complex cations $[(CO)_5M(Se_4)M(CO)_5]^{2+}$ (M = Mo, W), in which a rectangular Se_4^{2+} ion is coordinated on two opposite edges by $M(CO)_5$ fragments (15). The corresponding reaction with Te_4^{2+} yields $[(CO)_4M(Te_3)]^+$ (M = Mo, W) with a triangular Te_3^+ ligand bound to the metal atom via an η^3–π fashion (16). The structure of $Nb_3OTe_8I_7$ contains $[(Te_4)Nb_3O(Te_2)_2I_6]^+$ cations, in which an almost square planar Te_4^{2+} ion is coordinated to a trinuclear Nb_3O cluster (17). Compounds consisting of E_4^{2+} (E = S, Se, Te) cations and halogenometallate anions show a typical coordination of the cation by halogen atoms of the anions that bridge the edges of the E_4 ring (18). The closest Te · · · · · Br contacts in the structure of $MoTe_6Br_3$ are formed by Br^- anions that are located in the plane and over the edges of the Te_4 rings, which supports the assumption of Te_4^{2+} cations. Some of these Te · · · · · Br distances are very short. The distances Te(3)–Br(1) 282.8(1) and Te(5)–Br(2) 279.4(1) pm are close to the range of covalent Te–Br bonds that are observed at about 250 pm. If these two contacts are regarded as covalent bonds, a formally neutral Te_4Br_2 ring results. A molecular form of the tellurium subhalide Te_2Br is not known so far. The short Te · · · · Br contacts are responsible for the distortion of the Te_4 rings in complex I. Te · · · · · Br contacts in complex II are more equally distributed and are longer than 315 pm with the effect that the geometry of the Te_4 ring is undistorted and close to a square. The large number of short and considerably bonding Te · · · · · Br contacts gives rise to the interpretation of the structure of $MoTe_6Br_3$ as being built of cationic complexes $[Mo_2(Te_2)_2(Te_4)_2]^{6+}$ that are connected by bromide ions to layers (Fig. 4).

The complex cations in the structure of $MoTe_6Br_3$ can be considered as fragments of the one-dimensional chains in the structure of $MoTe_4Br$ (Fig. 5). If one starts from the point of ionic Te–Br bonds and Mo^{5+} in $MoTe_4Br$, the excision of a suitable chain fragment leads to $[(Mo^{5+})_2(Te_2^{2-})_6]^{2-}$. Withdrawing of eight electrons from this fragment leads to $[(Mo^{3+})_2(Te_2^{2-})_2(Te_4^{2+})_2]^{6+}$ and the formation of Te–Te bonds between four of the Te_2^{2-} groups and the simultaneous transition of Mo^{5+} to Mo^{3+}.

ACKNOWLEDGMENTS

Financial support by the Deutsche Forschungsgemeinschaft and the Fonds der Chemischen Industrie is gratefully acknowledged.

REFERENCES

1. J. Fenner, A. Rabenau, and G. Trageser, *Adv. Inorg. Chem. Radiochem.* **23,** 329 (1979).
2. C. Perrin, M. Sergent, F. LeTraon, and A. LeTraon, *J. Solid State Chem.* **25,** 197 (1978).
3. M. Sergent, O. Fischer, M. Decroux, C. Perrin, and R. Chevrel, *J. Solid State Chem.* **22,** 87 (1977).
4. J. Beck, *Angew. Chem.* **106,** 172 (1994); *Angew. Chem. Int. Ed. Engl.* **33,** 163 (1994).
5. B. E. Brown, *Acta Crystallogr.* **20,** 268 (1966).
6. R. Kniep, D. Mootz, and A. Rabenau, *Z. Anorg. Allg. Chem.* **422,** 17 (1976).
7. G. M. Sheldrick, "SHELXS 86, Program for Crystal Structure Determination." University of Göttingen, Germany, 1986.
8. G. M. Sheldrick, "SHELXL 93, Program for Crystal Structure Refinement," University of Göttingen, Germany, 1993.
9. *Caution:* Tellurium and liquid bromine react vehemently. It is recommended to fill the ampoule first with bromine, freeze it with liquid N_2, add tellurium powder, evacuate, and seal the ampoule, which then must be thawed very slowly and kept in an ice bath at 0°C until the reaction ceases.

10. W. Tremel, *Chem.Ber.* **125,** 2165 (1992).
11. With Pauling's formula (12) for the estimation of a bond order $d(n) = d(1) - 71$ pm log n one obtains for a 303 pm Te–Br bond and $d(1) = 250$ pm a bond order of 0.18.
12. L. Pauling, ''The nature of the chemical bond.'' Cornell University Press, Ithaca, N.Y., 1960.
13. G. Landrum, ''YAeHMOP, Program for eH Calculations''; for *k*-point settings see R. Ramirez and M. C. Böhm, *Int. J. Quantum Chem.* **34,** 571 (1988).
14. L. E. Bogan, T. B. Rauchfuβ, and A. L. Rheingold, *Inorg.Chem.* **24,** 3720 (1985).
15. M. J. Collins, R. J. Gillespie, J. W. Kolis, and J. F. Sawyer, *Inorg. Chem.* **25,** 2057 (1986); C. Belin, T. Makani, and J. Roziére, *J. Chem. Soc. Chem. Comm.* 118 (1985).
16. M. J. Collins, R. J. Gillespie, J. W. Kolis, and J. F. Sawyer, *Inorg. Chem.* **25,** 2057 (1986); A. Seigneurin, T. Makani, D. J. Jones, and J. Roziére, *J. Chem. Soc. Dalton Trans*. 2111 (1987).
17. W. Tremel, *J. Chem. Soc. Chem. Comm.* 126 (1992).
18. G. Cardinal, R. J. Gillespie, J. F. Sawyer, and J. E. Vekris, *J. Chem. Soc. Dalton Trans.* 765 (1982); J. J. Rothmann, L. S. Bartel, C. S. Ewing, and J. R. VanWazer, *J. Comput. Chem.* **1,** 64 (1980); J. Beck and G. Bock, *Z. Naturforsch.B* **51,** 119 (1996).